Brueckner-Hartree-Fock Calculations of Spherical Nuclei in a Harmonic-Oscillator Basis. III. Renormalized Calculations Using the Reid Potential*

K. T. R. Davies
Oak Ridge National Laboratory, Oak Ridge, Tennessee 37830

and

R. J. McCarthy†
Carnegie-Mellon University, Pittsburgh, Pennsylvania 15213
(Received 7 April 1971)

A G matrix derived from the Reid soft-core potential is used in a series of Brueckner-Hartree-Fock calculations of spherical nuclei. The G matrix is calculated using an intermediate-state spectrum and Pauli operator appropriate to pure oscillator orbitals, with options to shift the entire spectrum or the low-lying levels from unperturbed oscillator energies. The Pauli operator takes into account the filling of different neutron and proton subshells in $N \neq Z$ nuclei. Self-consistent occupation probabilities are included in the calculations and results are presented for ^{16}O, ^{40}Ca, ^{48}Ca, and ^{208}Pb. Various systematics and convergences are studied. Good results can be obtained for the binding energies, but the experimental binding energy and charge radius cannot be fitted simultaneously. It is shown that renormalization with occupation probabilities is crucial for calculating a reasonable single-particle spectrum. The difficulty of comparing single-particle energies with experiment is discussed with particular emphasis on heavy and superheavy nuclei. The nuclei ^{298}114 and ^{310}126 are calculated for a simple force.

I. INTRODUCTION

The present paper is a continuation and extension of the approach developed in a series of Hartree-Fock (HF),[1-4] Brueckner,[5] and Brueckner-Hartree-Fock (BHF)[6-8] calculations. The basic aim of these calculations is to start with a realistic nucleon-nucleon potential and calculate the total binding energy, radius, and single-particle (SP) parameters of spherical, doubly magic nuclei.

In the above references, and in all other calculations[9-22] based directly on realistic nucleon-nucleon interactions, the results obtained have been rather discouraging. All the nuclei studied have been underbound or too small. In addition, the calculations yield too low a level density for occupied SP states, especially in heavy nuclei. There are HF and BHF calculations[23-27] using effective interactions which do yield excellent agreement with experiment. An important feature of some of these effective interactions is the introduction of a density-dependent term in the two-body interaction. This term is important in yielding SP levels which agree with experiment and also tends to improve the saturation properties. However, most of the improvement in the binding energy and the charge radius is due to adjusting the strength and range of the interaction to obtain the desired saturation properties of nuclear matter or selected finite nuclei.

It is not clear whether the poor results obtained in Brueckner and BHF calculations are due to deficiencies in the two-body potential or to an inadequate many-body theory. It is clear, however, that the theory must be improved and that this can be done only by careful and systematic evaluation of higher-order Brueckner-Goldstone (BG) diagrams, using the best G matrices available. A study of the convergence of Brueckner theory is of particular importance.

Brueckner theory is basically a perturbation expansion, and the renormalized BHF (RBHF) formalism[28,19] used here includes a self-consistent treatment[7,8] of occupation probability diagrams in calculating the binding energy and SP energies. The importance of these diagrams has been shown previously[8,12,15,19,20] but this is the first large scale BHF calculation of medium and heavy nuclei in which these diagrams have been included in a self-consistent way. In Sec. II we discuss the general formalism of RBHF calculations, the BG diagrams involved, and the concept of occupation probability.

The calculation of the Brueckner reaction matrix G is outlined in Sec. III. The reaction matrices used are based on the Reid soft-core potential[29] for those partial waves in which the potential is defined and the Hamada-Johnston potential[30] for higher partial waves. Particular emphasis is placed on the choice of the intermediate-state spectrum used to define G, since this choice will determine the convergence properties of the BG expansion. Section IV contains brief discussions concerning details and notation of the RBHF

calculations, sources of numerical inaccuracy, and convergence with iteration.

Results are presented in Sec. V for the nuclei ^{16}O, ^{40}Ca, ^{48}Ca, and ^{208}Pb. The HF convergence with dimensionality is found to be satisfactory and, for a reasonable choice of intermediate-state spectrum, the results are almost independent of the oscillator parameter used to define the basis states. The effect of changing the intermediate-state spectrum is, however, quite large. In ^{40}Ca, for example, the binding energy per particle increases from 2.3 to 10.7 MeV and the charge radius decreases from 3.33 to 2.85 fm when the gap between occupied and unoccupied states is reduced by about 45 MeV.

Renormalized calculations are shown to yield consistently better saturation properties and SP energies than regular BHF calculations. In particular, renormalization is very important for obtaining a SP level density in ^{208}Pb which agrees with experiment. The comparison of calculated SP levels with experiment is, however, a complicated procedure[31] and becomes increasingly difficult in heavier nuclei. For superheavy nuclei these problems are especially critical. Another problem in heavy nuclei is that the energies of spin-unsaturated levels lie much too high.[13,4,6,32] For example, in ^{208}Pb, the calculated $0i_{13/2}$ neutron and $0h_{11/2}$ proton levels are separated from the other bound levels by a large gap. Renormalization does not correct this difficulty. However, it is interesting to note that this particular problem did not occur in a HF calculation of two superheavy nuclei. This is illustrated in the Appendix where we display the SP levels of ^{310}126 and ^{298}114, obtained using the Nestor force.[33]

In Sec. VI we summarize and review the results, pointing out those approximations which might be improved upon and some higher-order diagrams which should be evaluated. The choice of an intermediate-state spectrum remains the critical problem facing Brueckner theory. Although we are able to find a prescription for choosing the spectrum which yields reasonable binding energies for all the nuclei studied, we are not able to fit the binding energies and charge radii simultaneously. This defect might be alleviated by using renormalized wave functions to calculate the charge radius.

II. THEORY

As pointed out earlier, the RBHF formalism is a technique for summing certain classes of BG diagrams. We begin by choosing a harmonic-oscillator basis to define a set of SP wave functions $|\alpha\rangle$ and energies ϵ_α. The first-order approximation to the energy is then given by

$$E = \sum_\alpha{}' \langle \alpha | T | \alpha \rangle + \tfrac{1}{2} \sum_{\alpha,\beta}{}' \langle \alpha\beta | G(\omega = \epsilon_\alpha + \epsilon_\beta) | \alpha\beta \rangle , \tag{2.1}$$

where each G matrix element is antisymmetrized and primed summations go over occupied SP states only. This approximation to E sums the BG diagrams shown in Fig. 1(a).

We improve on this approximation by demanding Brueckner self-consistency in the starting energy ω. The total energy in the Brueckner approximation is given by

$$E = \sum_\alpha{}' \langle \alpha | T | \alpha \rangle + \tfrac{1}{2} \sum_{\alpha,\beta}{}' \langle \alpha\beta | G(\omega = E_\alpha + E_\beta) | \alpha\beta \rangle , \tag{2.2}$$

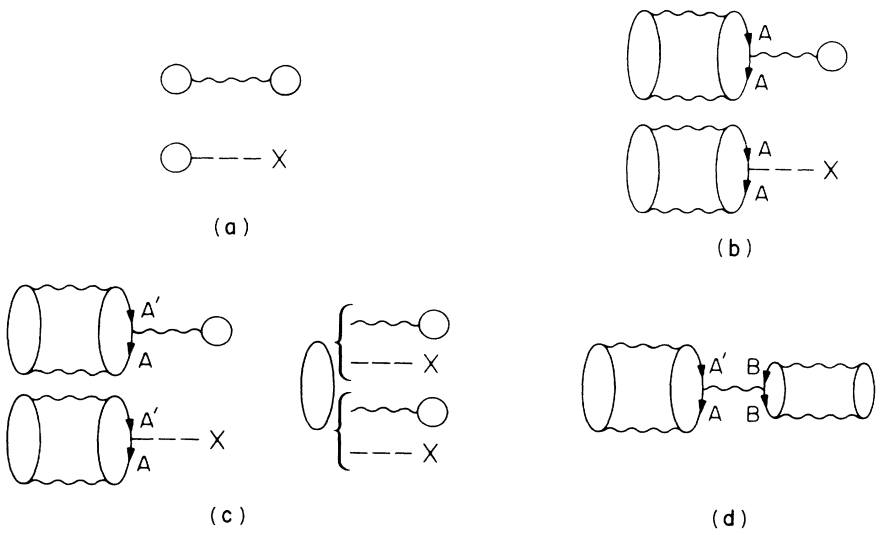

FIG. 1. Lowest-order diagrams summed in a RBHF calculation. Wavy lines signify G matrix interactions while dashed lines terminated by an × signify negative SP potential insertions.

where

$$E_\alpha = \langle \alpha | T | \alpha \rangle + \sum_\beta {}' \langle \alpha\beta | G(E_\alpha + E_\beta) | \alpha\beta \rangle . \quad (2.3)$$

Introducing this self-consistent SP potential for occupied states cancels the diagrams shown in Fig. 1(b) along with all higher-order diagrams with diagonal bubble or potential insertions in hole lines.[34,35] At the same time we change the first-order contribution to E since we have redefined the energies of the occupied states.

The BHF formalism cancels additional diagrams, namely the off-diagonal hole-hole and particle-hole diagrams shown in Fig. 1(c). The occupied-state wave functions must be eigenstates of a one-body BHF potential U which has hole-hole and particle-hole matrix elements defined as[35]

$$\langle A | U | A' \rangle = \sum_B \langle AB | \tfrac{1}{2}[G(E_A + E_B) + G(E_{A'} + E_B)] | A'B \rangle , \quad (2.4)$$

$$\langle A | U | a \rangle = \sum_B \langle AB | G(E_A + E_B) | aB \rangle . \quad (2.5)$$

Here capital letters refer to occupied BHF orbitals, while lower case letters, to unoccupied BHF orbitals. The occupied-state energies are again given by the Brueckner self-consistency condition of Eq. (2.3) with α, β replaced by A, B. Since the BHF wave functions are expanded in terms of a limited number of oscillator wave functions,

$$|A\rangle = \sum_\alpha |\alpha\rangle \langle \alpha | A \rangle , \quad (2.6)$$

the particle-hole diagrams are canceled only for those low-lying particle states which are included in the HF space.

Equations (2.4) and (2.5) do not completely specify the one-body BHF potential. In order to solve the BHF equations we must define the particle-particle matrix elements of U. The diagrams in Fig. 1(c) are canceled for any choice of $\langle a | U | a' \rangle$ but, in an exact BHF calculation, the occupied orbitals and total energy would depend on the particle-particle prescription chosen. The usual HF procedure is to choose the particle potential to cancel the particle-bubble diagrams shown in Fig. 2. However, in BHF calculations the middle G matrix in the particle-bubble insertion must be evaluated off the energy shell.[34] A proper self-consistent treatment of these diagrams is possible[36,37] but quite complicated, since the particle-particle matrix element of U depends on the excitation energy of the rest of the diagram.

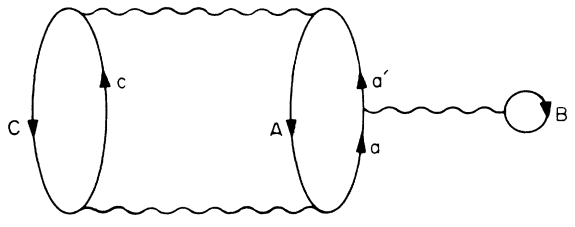

FIG. 2. The third-order particle-bubble diagram in which the middle G interaction must be evaluated off-energy shell.

Because of the complications involved, and also because it is not clear that these diagrams should not be treated as part of a larger class of three-body diagrams, we do not treat the particle-state energies self-consistently. We define the particle-particle matrix elements of U as[6,7]

$$\langle a | U | a' \rangle = \sum_B \langle aB | \tfrac{1}{2}[G(\bar{E}_a + E_B) + G(\bar{E}_{a'} + E_B)] | a'B \rangle , \quad (2.7)$$

where $\bar{E}_a$ could be chosen to take into account the off-shell behavior of the particle-bubble diagram in some average way. In the calculation presented here we can in fact choose the matrix elements $\langle a | U | a' \rangle$ completely arbitrarily with no effect on our results.[7] The reason for this is that we make two approximations in the calculations which combine to decouple the matrix elements $\langle a | U | a' \rangle$ from our results. The first approximation consists of using a Pauli operator defined in terms of pure oscillator orbitals rather than BHF orbitals. The second is that, in calculating G, we define the energies of the intermediate-state spectrum once and for all at the beginning of the calculation and hence do not treat the spectrum self-consistently.

It should be emphasized that, even though the prescription chosen to define $\langle a | U | a' \rangle$ does not affect the resulting binding energy or occupied BHF orbitals, it is necessary to choose some prescription in order to solve the BHF equations. The occupied-state orbitals are not known *a priori*, and it is only when self-consistency is reached that the occupied orbitals are uncoupled from the unoccupied BHF orbitals.[7] It should be reiterated, however, that the results do depend strongly on the type of intermediate spectrum used to evaluate G matrix elements.

The RBHF formalism cancels additional diagrams. Including occupation probabilities in the definition of the SP potentials cancels a large class of diagrams[28] of the type shown in Fig. 1(d). The final expression for the binding energy is[28,19]

$$E = \sum_A \langle A | T | A \rangle + \tfrac{1}{2} \sum_{A,B} \langle AB | G(E_A + E_B) | AB \rangle P_A P_B + \sum_A (1 - P_A) \langle A | U | A \rangle , \quad (2.8)$$

where

$$\langle A | U | A \rangle = \sum_B \langle AB | G(E_A + E_B) | AB \rangle P_B , \quad (2.9)$$

and[8]

$$P_A = \left[1 - \sum_B \langle AB | \frac{\partial G(\omega)}{\partial \omega} | AB \rangle P_B \right]^{-1} . \qquad (2.10)$$

In the above equations, each G matrix is evaluated on the energy shell with self-consistent starting energy ω, and the derivative in Eq. (2.10) is evaluated at the same value of ω. These equations reduce to the usual BHF equations when the occupation probabilities P_A are all set equal to unity.

The importance of the occupation probability diagrams depends on the strength of the nucleon-nucleon interaction v. If v were weak enough that $G(\omega)$ could be replaced by v, the occupation probabilities [see Eq. (2.10)] would all be unity and the HF procedure alone would be sufficient. Once the potential is strong enough that a BHF calculation is needed, the occupation probability diagrams should also be included.

In the preceding paragraphs we have discussed separately the three self-consistencies satisfied in a RBHF calculation. This separation is, of course, an artificial one, since Brueckner self-consistency, HF self-consistency, and occupation probability self-consistency are coupled together in the RBHF equations[7] and must all be satisfied simultaneously.

III. CALCULATION OF G AND CHOICE OF INTERMEDIATE-STATE SPECTRUM

The defining equation for G is written in operator form as

$$G(\omega) = v + v \frac{Q}{\omega - H_{ab}} G(\omega) , \qquad (3.1)$$

where v is the nucleon-nucleon interaction, Q forbids scattering into occupied SP states, H_{ab} is a two-particle Hamiltonian defining the intermediate-state spectrum, and the starting energy ω is a parameter to be determined through Brueckner self-consistency. We evaluate matrix elements of G first in the relative-center-of-mass (RCM) harmonic-oscillator representation. These matrix elements are then transformed into the SP oscillator representation, and matrix elements of G in the BHF representation are expressed as linear combinations of oscillator matrix elements.

Since we are evaluating G in the RCM representation we cannot treat the Pauli operator Q exactly. We use an approximate "angle averaged" Q[12,5] appropriate to pure oscillator orbitals which is diagonal in the RCM oscillator representation. No attempt is made to treat Q self-consistently in the BHF procedure. We do, however, take into account the fact that the number of occupied SP states is different for protons and neutrons in $N \neq Z$ nuclei. There we obtain three sets of relative G matrix elements corresponding to neutron-neutron, proton-proton, and neutron-proton interactions. We also show in Sec. V that little change is introduced by using the neutron-proton Pauli operator for all three cases. The over-all error due to our approximate treatment of Q is probably quite small. It has been shown many times[12,38] that the angle averaged Q used here is a good approximation for pure Brueckner calculations, and the additional error introduced by not using a self-consistent BHF Q should be quite small if the oscillator states used to define Q have large overlaps with the resulting BHF orbitals.

The major source of uncertainty in the theory lies in the choice of H_{ab}, the intermediate-state Hamiltonian. The definition of H_{ab} is in principle arbitrary, since the BG expansion is valid for any choice of basis states and energies. The choice of H_{ab} will, however, drastically affect the convergence of the BG expansion and yield substantially different results for the RBHF calculation, which is a truncation of this expansion. This simply means that the contribution of diagrams not included in the RBHF formalism depends strongly on the choice of intermediate-state spectrum, and we should in principle choose H_{ab} to minimize the effects of these higher-order diagrams.

Our basic definition for H_{ab} is[11,5]

$$H_{ab} = H_{osc} - 2C - \sum_{\alpha,\beta} 2B_0 |\alpha\beta\rangle\langle\alpha\beta| , \qquad (3.2)$$

where

$$H_{osc} = \frac{1}{2m}(p_\alpha^2 + p_\beta^2) + \tfrac{1}{2} m\Omega^2 (r_\alpha^2 + r_\beta^2) , \qquad (3.3)$$

and $|\alpha\beta\rangle$ is a two-particle oscillator wave function. The sum over intermediate states is truncated such that all two-particle states with

$$2n_\alpha + l_\alpha + 2n_\beta + l_\beta = 2n + l + 2N + L \leq \bar{N} - 4 \qquad (3.4)$$

are shifted by an amount $2B_0$, while the higher-lying states are unshifted. This parametrization of H_{ab} enables us to transform easily to the RCM representation and also lets us shift either the entire spectrum or the low-lying two-particle states separately from the higher states.

This definition of H_{ab} might seem in conflict with our assumption of an underlying set of SP wave functions and energies on which the BG expansion is based. This is not true. Our basis set of wave functions is still defined by a harmonic-oscillator Hamiltonian. We have simply changed the *energies* of all two-particle intermediate states in order to cancel, in some average sense, the effect of higher-order diagrams. It was pointed out in the previous section that the G matrices involved in higher-order diagrams (e.g., the third-order

particle-bubble diagram of Fig. 2) must be evaluated off the energy shell and any particle-state potential defined to cancel these diagrams would depend on the excitation energy of the entire diagram. Thus, the intermediate-state Hamiltonian should *not* necessarily be written as the sum of two SP Hamiltonians but rather as some function of the product state.

The procedure used in calculating G matrix elements has been discussed earlier[5] and we review it here very briefly. The operator $G(\omega)$ is expressed in terms of a simpler reference operator $G_R(\omega)$ as[34]

$$G(\omega) = G_R(\omega) + G_R(\omega)\left[\frac{Q}{\omega - H_{ab}} - \frac{1}{\omega - H_R}\right]G(\omega), \tag{3.5}$$

where

$$G_R(\omega) = v + v\frac{1}{\omega - H_R}G_R(\omega) \ . \tag{3.6}$$

Here H_R is a reference two-particle Hamiltonian which we choose to be of the form

$$H_R = H_{\rm osc} - 2C \ .$$

The equation for $G_R(\omega)$ separates easily into RCM harmonic-oscillator states and is diagonal in the center-of-mass quantum numbers. For a given choice of oscillator frequency Ω, we calculate all necessary G_R matrix elements for a mesh of ω values. These matrix elements need be calculated only once.

Matrix elements of $G(\omega)$ are found by matrix inversion[15] of Eq. (3.5). This operation must be carried out separately for each nucleus (since Q depends on the particular nucleus under consideration) and for each distinct choice of the parameters B_0 and $\bar{N}$. The size of the matrix inversion is usually determined by the value chosen for $\bar{N}$. In those cases where $\bar{N}$ (or B_0) is zero, the size of the matrix is governed by how fast the operator $Q - 1$ goes to zero.

Results are presented for a variety of choices of intermediate-state spectrum. There is as yet no precise prescription for picking "best" values for B_0, C, and $\bar{N}$. However, the best results are obtained by choosing B_0 and C such that the low-lying intermediate-state spectrum starts near zero energy. This is encouraging, since it gives a physically reasonable picture[35] of the effective one-body potential.

IV. BHF DETAILS AND NOTATIONS

Two-body G matrix elements are computed from the relative matrix elements described in the previous section, using formula (10) of Tarbutton and Davies.[4] The matrix elements converge very quickly with relative l and, for all calculations presented in this paper, we truncate at relative f waves, i.e.,

$$l_{\rm rel}^{(\max)} = 3. \tag{4.1}$$

This truncation has no significant effect on our results, even for heavy nuclei.[4,6]

We use a four-point Lagrangian interpolation scheme to find G as a function of the starting energy ω. Thus each two-body matrix element is stored in the computer as four numbers G_0, G_1, G_2, and G_3 and, while iterating, we evaluate $G(\omega)$ from the expression

$$G(\omega) = G_0 + \omega G_1 + \omega^2 G_2 + \omega^3 G_3 \ . \tag{4.2}$$

The same coefficients can simultaneously be used to calculate

$$\frac{\partial G}{\partial \omega} = G_1 + 2\omega G_2 + 3\omega^2 G_3 \ , \tag{4.3}$$

which is substituted into Eq. (2.10) to obtain the occupation probabilities.

The interpolation points used to find the coefficients G_0, G_1, G_2, and G_3 were chosen to cover the ω region of physical interest as well as possible. However, interpolation is still a significant source of numerical inaccuracy, particularly with respect to the occupation probabilities. We have found that modifications of the interpolation scheme which change the SP energies in the third or fourth significant figure cause the occupation probabilities to change in the second or third significant figure.

Another computational problem is the convergence of the BHF results with iteration. The double self-consistency has an interesting effect on the calculated quantities. There is a variational principle on the energy in pure HF calculations, and the SP energies converge with iteration in a *monotonic* fashion. In a pure Brueckner calculation the energies *oscillate* with iteration. The oscillatory behavior can be understood from the following rough argument. We denote the "true" ω value by ω_0 and for values of ω close to ω_0

$$G(\omega_I) \approx G(\omega_0) + \left(\frac{\partial G}{\partial \omega}\right)_{\omega=\omega_0}(\omega_I - \omega_0) \ , \tag{4.4}$$

where ω_I is the ω value for iteration I. The SP energies used to calculate ω_I are results of the *previous* iteration. The derivative in Eq. (4.4) is negative for most matrix elements of significance, so that if $\omega_I > \omega_0$ then $G(\omega_I) < G(\omega_0)$. This means that the SP levels calculated for iteration I are too attractive, i.e., $\omega_{I+1} < \omega_0$, so that $G(\omega_{I+1}) > G(\omega_0)$, etc. The more we shift the intermediate-

particle spectrum, the steeper the $G(\omega)$ curve and the more severe the fluctuations. For large shifts of the spectrum, many iterations may be required to achieve self-consistency, a result shown in Table I for an $I = 50$ calculation. This table also demonstrates that the convergence can be dramatically improved by *averaging* the SP energies from the two previous iterations. Therefore, in any Brueckner calculation some type of energy averaging should always be used to reduce the number of iterations. Finally, whether HF convergence (monotonic behavior) or Brueckner convergence (oscillations) dominates in a BHF calculation depends upon the magnitude of $\partial G/\partial\omega$, which in turn depends upon how much the intermediate spectrum is shifted.

Convergence with iteration is also affected by the off-shell value one used for $\bar{E}_a$ in Eq. (2.7).[7] Two examples are

$$\bar{E}_a = 2E^{(\mathrm{ave})} - E_a \,, \tag{4.5}$$

where $E^{(\mathrm{ave})}$ is the average of all occupied SP energies, and

$$\bar{E}_a = E_a \,, \tag{4.6}$$

which is the on-shell value. Prescription (4.6) converges with iteration faster than Eq. (4.5) and since both prescriptions yield the same occupied states,[7] it would seem preferable to use Eq. (4.6). However, the unoccupied SP energies do depend on the off-shell prescription, and for our calculations we use Eq. (4.5), since it gives a better approximation to the particle-bubble diagram. The energy denominator of the middle G matrix in Fig. 2 is

$$\omega - H_{12} = E_B + E_A + E_C - E_c - H_{12} \,, \tag{4.7}$$

TABLE I. Convergence with iteration for pure Brueckner calculations of ^{16}O with $\hbar\Omega = 12.5$, $C = 0$, $\bar{N} = 18$, and $B_0 = \frac{7}{2}\hbar\Omega$. The numbers in parentheses are from a calculation in which the SP energies to be used in each iteration are averages of the values obtained in the *two* previous iterations. The numbers shown are typical of other SP energies and occupation probabilities. The $0s_{1/2}$ neutron energies are in MeV.

Number of iterations	$E_{0s_{1/2}(\mathrm{neutron})}$	$P_{0p_{1/2}(\mathrm{neutron})}$
5	−31.108 (−32.337)	0.80 725 (0.79 656)
10	−32.627 (−32.168)	0.79 324 (0.79 750)
15	−31.990 (−32.177)	0.79 913 (0.79 739)
20	−32.256 (−32.178)	0.79 666 (0.79 739)
25	−32.145	0.79 770
30	−32.191	0.79 726
40	−32.180	0.79 737
50	−32.178	0.79 739

which we approximate by

$$E_B + \bar{E}_a - H_{12} \,.$$

Obviously, the simplest average value for $\bar{E}_a$ is given by Eq. (4.5).

In a HF-type calculation in the oscillator representation, a SP dimensionality must be chosen. Let d_s be the dimensionality of all states having the same *symmetry type*[4] s,

$$s \equiv (q, l, j) \,, \tag{4.8}$$

where q is the charge, l is the orbital angular momentum, and j is the total angular momentum. We then define a "total dimensionality" D for the whole calculation. If all symmetry types have the same number of occupied states, e.g., ^{4}He and ^{16}O, then all d_s have the same constant value d and we have

$$D = d \,. \tag{4.9}$$

However, for nuclei such as ^{40}Ca, ^{48}Ca, and ^{208}Pb in which each symmetry type has a different number of occupied states, it is convenient to define[4]

$$D = P + \delta \,, \tag{4.10a}$$

if

$$d_s = \eta_s + \delta \,, \tag{4.10b}$$

where η_s is the number of occupied states of symmetry type s. The notation P in Eq. (4.10a) stands for "pure oscillator"; thus δ tells us how many wave functions beyond a pure oscillator basis are being used. For calculations of unoccupied symmetry types, e.g., the d states in ^{16}O, it is also convenient to adopt the notation

$$D_o \equiv \text{total dimensionality of the } \textit{occupied} \text{ symmetry types} \,, \tag{4.11a}$$

$$D_u \equiv \text{total dimensionality of the } \textit{unoccupied} \text{ symmetry types} \,. \tag{4.11b}$$

(In the last case $\eta_s = 0$ for each type considered.)

The total energy is calculated from Eq. (2.8), and the mass, proton, and neutron rms radii from the following formulas:

$$r_m^2 = \mathrm{Tr}(r^2\rho)/A, \tag{4.12a}$$

$$r_p^2 = \mathrm{Tr}(r^2\rho_p)/Z \,, \tag{4.12b}$$

$$r_n^2 = \mathrm{Tr}(r^2\rho_n)/N, \tag{4.12c}$$

where ρ is the one-body density; A, Z, and N are the total numbers of nucleons, protons, and neutrons. We also compute a *charge* radius r_c,

$$r_c^2 = r_p^2 + r_{\mathrm{prot}}^2 \,, \tag{4.13}$$

where r_{prot} is the finite size of the proton. In all of the results of this paper we take $r_{\mathrm{prot}}^2 = 0.64$

fm^2. Unless otherwise specified, the results also contain center-of-mass corrections on the total energy and the various rms radii. For the energy and mass radius, the corrected values are given by[39]

$$E' = E - \langle P^2 \rangle / 2Am\,, \tag{4.14a}$$

$$r_m'^2 = r_m^2 - \langle R^2 \rangle\,, \tag{4.14b}$$

where $\vec{P}$ and $\vec{R}$ are the center-of-mass momentum and radius, m is the nucleon mass, and the brackets denote expectation values. The corrections to the neutron and proton radii are a bit more complicated and are discussed in detail by Davies and Becker.[39]

V. RESULTS

Separate results will be presented for ^{16}O, ^{40}Ca, ^{48}Ca, and ^{208}Pb. The major effects studied include the following: (a) variation of the results as a function of $\hbar\Omega$; (b) variation as a function of the parameters B_0, C, and $\bar{N}$, which define the intermediate-state spectrum used in evaluating G; (c) differences between calculations with self-consistent and unit occupation probabilities; and (d) convergence with dimensionality of the SP representation. Since most of these effects are quite similar in all of the nuclei studied, different effects will be emphasized for each nucleus. In addition, in ^{208}Pb we will discuss in some detail the special problems associated with the SP spectra of heavy nuclei.

A. ^{16}O

The SP energies and occupation probabilities, the binding energy per nucleon, and the rms mass, neutron, and charge radii are shown in Table II as a function of $\hbar\Omega$. The parameters $\bar{N} = 18$, $C = 0$, and $B_0 = \frac{7}{2}\hbar\Omega$ indicate that, in calculating G matrix elements, all intermediate product states with $2n_1 + l_1 + 2n_2 + l_2 + 4 \leq 18$ have been lowered by $7\hbar\Omega$. For this particular choice of B_0 the intermediate-state spectrum starts at zero energy. Our choice of $\bar{N} = 18$ for ^{16}O corresponds roughly to the nuclear-matter argument[37] that the energies of all intermediate states between k_F and $2k_F$ should be lowered. In applying this argument to finite nuclei we choose to count the number of major oscillator shells involved. There is, of course, nothing unique about our prescription for either B_0 or $\bar{N}$ and we will be presenting results

TABLE II. BHF calculations of ^{16}O. For each case, a dimensionality of 6 is used with $C = 0$ and $\bar{N} = 18$. Energies are in MeV here and all remaining tables of the paper.

$\hbar\Omega$	9.5	11.0	12.5		14.0		15.5
$B_0/\hbar\Omega$	3.5	3.5	3.0	3.5	3.0	3.5	3.5
Neutrons							
$E_{0s_{1/2}}$	−36.8	−36.8	−37.4	−36.9	−37.4	−37.0	−37.4
$E_{0p_{3/2}}$	−18.4	−18.3	−17.5	−18.3	−17.3	−18.2	−18.3
$E_{0p_{1/2}}$	−15.6	−15.5	−14.3	−15.3	−14.0	−15.2	−15.1
$P_{0s_{1/2}}$	0.81	0.81	0.85	0.82	0.85	0.82	0.82
$P_{0p_{3/2}}$	0.79	0.78	0.83	0.78	0.83	0.78	0.78
$P_{0p_{1/2}}$	0.78	0.78	0.82	0.78	0.83	0.78	0.78
Protons							
$E_{0s_{1/2}}$	−34.2	−34.1	−34.5	−34.2	−34.5	−34.3	−34.7
$E_{0p_{3/2}}$	−15.9	−15.8	−14.8	−15.8	−14.6	−15.7	−15.7
$E_{0p_{1/2}}$	−13.2	−13.0	−11.7	−12.9	−11.4	−12.7	−12.6
$P_{0s_{1/2}}$	0.81	0.81	0.84	0.81	0.85	0.82	0.82
$P_{0p_{3/2}}$	0.78	0.78	0.83	0.78	0.83	0.78	0.78
$P_{0p_{1/2}}$	0.78	0.78	0.82	0.77	0.83	0.77	0.78
$-E/A$	6.76	6.65	5.52	6.57	5.33	6.49	6.47
r_m (fm)	2.46	2.45	2.46	2.44	2.46	2.43	2.41
r_n (fm)	2.45	2.44	2.45	2.43	2.45	2.42	2.41
r_c (fm)	2.59	2.59	2.60	2.57	2.60	2.57	2.55

for a variety of choices. In Table II, for example, two cases are shown for $B_0 = 3\hbar\Omega$.

The dependence of the results on $\hbar\Omega$ is not due to poor HF convergence. This is clear from Fig. 3 which shows the convergence with dimensionality of the charge radius for a number of $\hbar\Omega$ values. This convergence is typical of that for all the results in Table II. The $\hbar\Omega$ dependence is due partly to the fact that the calculations are not completely self-consistent (e.g., an oscillator Q is used in calculating G), but is probably due mainly to higher-order diagrams not taken into account.

The intermediate-state spectrum should be chosen to cancel higher-order diagrams as well as possible. If the BG expansion were summed to infinite order the results would be completely independent of $\hbar\Omega$. Thus a necessary (but obviously not sufficient) requirement for an intermediate-state spectrum is that it yield results independent of $\hbar\Omega$. We see in Table II that the results for B_0 in the vicinity of $\frac{7}{2}\hbar\Omega$ are almost independent of $\hbar\Omega$.

Comparing the results obtained with $B_0 = 3\hbar\Omega$ and $B_0 = 3.5\hbar\Omega$ we see that, as the intermediate-state spectrum is lowered, the binding energy increases, the rms radii decrease, the occupation probabilities decrease, and most of the SP states become slightly more bound. The SP energies are much less sensitive to shifts in the spectrum than in calculations with unit occupation probabilities.[8] This stability can be explained by the following argument. Lowering the intermediate-state spectrum makes the G matrix elements more attractive, which tends to lower the occupied SP energies. However, the changes in the occupied SP energies are smaller than the shift in the intermediate-state spectrum which caused them. This results in a reduced gap between occupied and unoccupied states, leading to more virtual excitations and smaller occupation probabilities. Decreasing the occupation probabilities raises the SP energies [see Eq. (2.9)], thus partially cancelling the original lowering effect. In fact, in our calculations the $0s_{1/2}$ states actually become more repulsive as B_0 is increased.

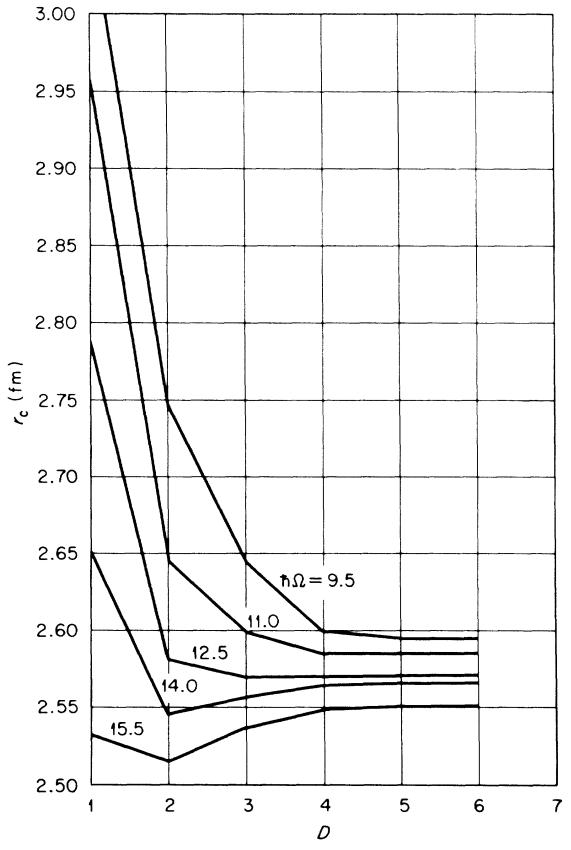

FIG. 3. ^{16}O charge radius r_c as a function of dimensionality D, for various $\hbar\Omega$ values. The intermediate-state parameters are $\bar{N} = 18$, $C = 0$, and $B_0 = \frac{7}{2}\hbar\Omega$.

All results shown in Table II are obtained using a SP dimensionality $D = 6$, which is more than adequate for ^{16}O. From Fig. 3 we see that for $\hbar\Omega = 11.0$, 12.5, and 14.0, satisfactory convergence is obtained for $D = 3$ and, for all $\hbar\Omega$ values, good convergence for $D = 4$. The figure does illustrate the importance of picking a reasonable $\hbar\Omega$ value if one is limited to rather small dimensionalities. This problem is of critical importance in heavy nuclei where the dimensionalities have to be much more severely restricted.[6]

B. ^{40}Ca and ^{48}Ca

Results for ^{40}Ca and ^{48}Ca are displayed in Table III. The Pauli operator for ^{48}Ca properly takes into account that the $0f_{7/2}$ state is occupied with neutrons but not protons. The first three columns show that $\hbar\Omega = 12.5$ gives reasonable convergence with dimensionality for the occupied states. The unoccupied SP energies, which are underlined, do not converge very well, but this is an expected problem which plagues all HF calculations performed in the oscillator representation.[2,3] Notice that the dimensionality of the occupied states varies according to the symmetry type, as described in Sec. IV. Also, as mentioned previously, different values can be obtained for the excited-state energies by picking a different prescription for $\bar{E}_a$.

The columns with asterisks are for calculations with unit occupation probabilities. Thus Table III also shows a comparison between renormalized and unrenormalized results. A comparison of the density distributions for the two kinds of calculations is presented in Fig. 4. The effects of including self-consistent occupation probabilities are to

TABLE III. BHF calculations of ^{40}Ca and ^{48}Ca for $\hbar\Omega = 12.5$, $B_0/\hbar\Omega = 4.0$, $C = 0$, and $\bar{N} = 20$. The first three columns show the convergence with dimensionality in ^{40}Ca; the columns with an asterisk are for unrenormalized calculations. D_o is the dimensionality of occupied symmetry types; D_u, of unoccupied symmetry types. The particle-particle prescription used is $\bar{E}_a = 2E^{(\mathrm{ave})} - E_a$; excited states are underlined.

Nucleus	^{40}Ca	^{40}Ca	^{40}Ca	^{40}Ca*	^{48}Ca	^{48}Ca*
D_o	$P+2$	$P+3$	$P+4$	$P+3$	$P+4$	$P+3$
D_u	3	4	5	4	5	4
Neutrons						
$E_{0s_{1/2}}$	−55.01	−54.83	−54.81	−68.2	−54.8	−68.6
$E_{0p_{3/2}}$	−35.20	−35.13	−35.12	−45.3	−35.8	−46.4
$E_{0p_{1/2}}$	−32.42	−32.41	−32.40	−41.4	−34.7	−44.7
$E_{0d_{5/2}}$	−17.51	−17.50	−17.49	−24.7	−18.1	−25.4
$E_{1s_{1/2}}$	−15.86	−15.84	−15.82	−21.8	−16.7	−22.9
$E_{0d_{3/2}}$	−13.38	−13.41	−13.41	−18.8	−16.3	−22.5
$E_{0f_{7/2}}$	3.55	3.26	3.14	0.54	−2.1	−6.5
$E_{1p_{3/2}}$	3.68	2.55	1.88	1.1	0.70	−0.45
$E_{1p_{1/2}}$	5.05	3.64	2.80	2.7	1.4	0.80
$E_{0f_{5/2}}$	7.75	7.10	6.62	6.6	4.1	3.4
$P_{0s_{1/2}}$	0.8276	0.8286	0.8286	1.0	0.85	1.0
$P_{0p_{3/2}}$	0.8352	0.8357	0.8358	1.0	0.86	1.0
$P_{0p_{1/2}}$	0.8300	0.8306	0.8306	1.0	0.85	1.0
$P_{0d_{5/2}}$	0.8377	0.8382	0.8383	1.0	0.86	1.0
$P_{1s_{1/2}}$	0.8374	0.8386	0.8387	1.0	0.86	1.0
$P_{0d_{3/2}}$	0.8323	0.8327	0.8329	1.0	0.86	1.0
$P_{0f_{7/2}}$					0.90	1.0
Protons						
$E_{0s_{1/2}}$	−48.37	−48.22	−48.20	−59.8	−51.2	−62.9
$E_{0p_{3/2}}$	−28.91	−28.85	−28.84	−37.4	−33.3	−41.9
$E_{0p_{1/2}}$	−26.20	−26.21	−26.21	−33.6	−32.3	−40.4
$E_{0d_{5/2}}$	−11.55	−11.54	−11.54	−17.2	−16.0	−21.6
$E_{1s_{1/2}}$	−9.93	−9.94	−9.93	−14.3	−14.3	−19.0
$E_{0d_{3/2}}$	−7.54	−7.59	−7.59	−11.4	−14.7	−19.5
$E_{0f_{7/2}}$	9.77	9.25	8.97	8.4	5.5	4.9
$E_{1p_{3/2}}$	9.77	8.22	7.20	8.2	4.7	5.3
$E_{1p_{1/2}}$	11.00	9.11	7.89	9.4	5.2	6.4
$E_{0f_{5/2}}$	13.32	12.31	11.48	13.0	7.1	7.9
$P_{0s_{1/2}}$	0.8225	0.8233	0.8233	1.0	0.83	1.0
$P_{0p_{3/2}}$	0.8321	0.8325	0.8325	1.0	0.83	1.0
$P_{0p_{1/2}}$	0.8270	0.8275	0.8275	1.0	0.83	1.0
$P_{0d_{5/2}}$	0.8360	0.8366	0.8367	1.0	0.83	1.0
$P_{1s_{1/2}}$	0.8362	0.8376	0.8379	1.0	0.84	1.0
$P_{0d_{3/2}}$	0.8312	0.8318	0.8320	1.0	0.83	1.0
$-E/A$	4.980	4.993	4.994	4.21	4.00	3.30
r_n (fm)	3.036	3.046	3.048	2.90	3.41	3.21
r_c (fm)	3.178	3.190	3.193	3.05	3.25	3.11

raise the SP levels, to increase the rms radii, and to increase the binding energy, all of which tend to improve the agreement with experiment.

However, it is clear that, even with self-consistent occupation probabilities, the results still differ quite a bit from the experimental values. (For example, for ^{40}Ca the experimental binding energy[40] and charge radius[41] are 8.55 MeV and 3.50 fm, respectively.) The shift used in Table III for the low-lying spectrum is fairly moderate and we can obviously increase the binding energy by taking a larger shift, but this would have the effect of making the radius even smaller. This behavior is shown in Table IV, which presents the SP energies and occupation probabilities, the binding energy per nucleon, and the charge radius as a function of the parameters C, B_0, and $\bar{N}$ defined in Sec. III. The first column shows the results for a pure harmonic-oscillator intermediate-state spectrum. Comparing the second and third columns, we see the effect of changing B_0, the *magnitude* of the low-lying shift, while a comparison of the third and fourth columns demonstrates the effect of increasing $\bar{N}$, which gives roughly the *number* of low-lying states shifted. The last column shows the behavior when the entire excited-state spectrum is shifted by a constant amount C. The parameters $B_0 = \frac{9}{2}\hbar\Omega$ and $\bar{N} = 26$ used in column 4 again correspond roughly to lowering to zero energy the spectrum of intermediate states with momenta between k_F and $2k_F$. For this choice of parameters the nucleus is underbound by approximately 1.5 MeV, a result similar to that obtained in ^{16}O. Notice that for $C = B_0 = \bar{N} = 0$ the occupation probabilities tend to be greater at the top than at the bottom of the SP well, but as the spectrum is shifted this trend seems to be reversed. It is not certain yet whether this effect is real since, as mentioned in Sec. IV, numerical inaccuracy due to the interpolation scheme can cause the occupation probabilities to change in the second or third significant figure.

TABLE IV. BHF calculations of ^{40}Ca for $\hbar\Omega = 12.5$ and $D = P + 2$.

$C/\hbar\Omega$	0.0	0.0	0.0	0.0	4.5
$B_0/\hbar\Omega$	0.0	4.0	4.5	4.5	0.0
$\bar{N}$	0	20	20	26	0
Neutrons					
$E_{0s_{1/2}}$	−50.2	−55.0	−54.7	−58.2	−70.7
$E_{0p_{3/2}}$	−31.7	−35.2	−34.9	−37.5	−46.6
$E_{0p_{1/2}}$	−29.0	−32.4	−32.2	−34.5	−42.6
$E_{0d_{5/2}}$	−14.4	−17.5	−18.0	−19.7	−25.6
$E_{1s_{1/2}}$	−12.8	−15.9	−16.4	−17.9	−23.0
$E_{0d_{3/2}}$	−10.3	−13.4	−14.1	−15.5	−20.1
$P_{0s_{1/2}}$	0.88	0.83	0.82	0.81	0.80
$P_{0p_{3/2}}$	0.90	0.84	0.81	0.80	0.80
$P_{0p_{1/2}}$	0.90	0.83	0.81	0.79	0.79
$P_{0d_{5/2}}$	0.92	0.84	0.79	0.77	0.73
$P_{1s_{1/2}}$	0.92	0.84	0.79	0.77	0.72
$P_{0d_{3/2}}$	0.92	0.83	0.78	0.76	0.71
Protons					
$E_{0s_{1/2}}$	−43.2	−48.4	−48.4	−51.9	−64.2
$E_{0p_{3/2}}$	−24.9	−28.9	−28.9	−31.5	−40.5
$E_{0p_{1/2}}$	−22.4	−26.2	−26.3	−28.6	−36.6
$E_{0d_{5/2}}$	−7.9	−11.5	−12.4	−14.1	−20.0
$E_{1s_{1/2}}$	−6.4	−9.9	−10.9	−12.4	−17.5
$E_{0d_{3/2}}$	−4.1	−7.5	−8.6	−10.0	−14.7
$P_{0s_{1/2}}$	0.88	0.82	0.81	0.80	0.80
$P_{0p_{3/2}}$	0.90	0.83	0.81	0.80	0.79
$P_{0p_{1/2}}$	0.89	0.83	0.80	0.79	0.78
$P_{0d_{5/2}}$	0.92	0.84	0.78	0.77	0.72
$P_{1s_{1/2}}$	0.92	0.84	0.78	0.76	0.71
$P_{0d_{3/2}}$	0.92	0.83	0.77	0.75	0.70
$-E/A$	2.32	4.98	5.83	6.98	10.7
r_c (fm)	3.33	3.18	3.14	3.06	2.85

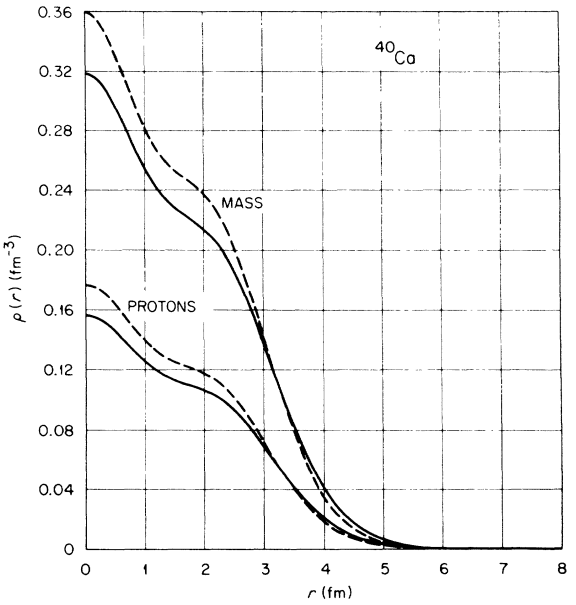

FIG. 4. Proton and mass densities of ^{40}Ca for $\hbar\Omega = 12.5$, $\bar{N} = 20$, $C = 0$, and $B_0 = 4\hbar\Omega$. The solid curves are for a renormalized calculation; the dashed curves, for an unrenormalized calculation.

By making various kinds of adjustments of the intermediate spectrum, we can bring the binding energy into agreement with experiment, but at the expense of making the radius too small. However, the radius does not change as drastically as the binding energy. (E.g., from Table IV we see that increasing B_0 from $4\hbar\Omega$ to $4.5\hbar\Omega$ changes the binding energy by 17%, but r_c by only 1%.) Also, the radius is not computed to the same accuracy as the binding energy; i.e., there are higher-order diagrams included in the binding energy which have not been calculated to the same order for the radius.

C. ^{208}Pb

A complete BHF calculation of ^{208}Pb is listed in Table V. Different B_0 and $\bar{N}$ values are used for each type of nucleon-nucleon interaction (i.e., proton-proton, neutron-proton, and neutron-neutron). Also, the Pauli operator properly takes into account the high-lying SP levels occupied by neutrons but not protons, so that there is a separate $1-Q$ for each nucleon-nucleon interaction. The numbers in parentheses are for an unrenormalized calculation, and we obtain the same kinds of results as for ^{40}Ca. Comparing the two kinds of calculations, we see that renormalization substantially raises all of the SP levels (the $0s_{1/2}$ neutron level, by 20 MeV) and increases the binding energy per nucleon by 1 MeV.

Additional binding can be obtained by lowering the intermediate-state spectrum, an effect demonstrated in Table VI. Only selected neutron SP energies and occupation probabilities are listed. Case A is the same as the calculation in Table V, while in the other cases each nucleon-nucleon interaction is obtained from the same intermediate spectrum and a neutron-proton Pauli operator (i.e., the neutron-neutron and proton-proton interactions are calculated with the same $(1-Q)$ and the same C, B_0, and $\bar{N}$ used for the neutron-proton interaction). Thus, the matrix elements for case B are derived from a Pauli operator and an intermediate spectrum which might be described as "averages" of the corresponding quantities used in case A. This kind of "averaging," which considerably simplifies the calculation, does not significantly change the results.

TABLE V. Calculations of ^{208}Pb for $\hbar\Omega = 9.5$, $C = 0$, and $D = P + 2$. The other intermediate-state parameters are $B_0/\hbar\Omega = 6.0$, 6.5, 7.0, and $\bar{N} = 26$, 27, 28 for proton-proton, neutron-proton, and neutron-neutron interactions, respectively. The values in parentheses are for an unrenormalized BHF calculation, with unit occupation probabilities.

SP states	Neutrons		Protons	
	SP energies	Occupation probabilities	SP energies	Occupation probabilities
$0s_{1/2}$	−71.1 (−91.1)	0.84	−58.6 (−72.5)	0.80
$0p_{3/2}$	−59.2 (−76.5)	0.84	−47.1 (−58.7)	0.80
$0p_{1/2}$	−58.8 (−75.8)	0.84	−46.9 (−58.2)	0.80
$0d_{5/2}$	−47.0 (−61.7)	0.84	−35.5 (−44.8)	0.80
$0d_{3/2}$	−46.7 (−61.0)	0.85	−35.4 (−44.4)	0.80
$1s_{1/2}$	−45.8 (−60.0)	0.84	−34.2 (−42.9)	0.80
$0f_{7/2}$	−34.7 (−46.8)	0.85	−23.7 (−30.7)	0.81
$0f_{5/2}$	−34.6 (−46.2)	0.85	−23.6 (−30.3)	0.81
$1p_{3/2}$	−32.8 (−44.1)	0.85	−21.6 (−27.8)	0.81
$1p_{1/2}$	−32.5 (−43.4)	0.85	−21.4 (−27.2)	0.80
$0g_{9/2}$	−22.5 (−32.0)	0.86	−11.9 (−16.7)	0.81
$0g_{7/2}$	−22.2 (−31.1)	0.85	−11.8 (−16.0)	0.81
$1d_{5/2}$	−20.1 (−28.8)	0.86	−9.4 (−13.2)	0.82
$1d_{3/2}$	−19.3 (−27.3)	0.86	−8.8 (−12.2)	0.81
$2s_{1/2}$	−19.3 (−27.2)	0.86	−8.6 (−11.7)	0.82
$0h_{11/2}$	−10.5 (−17.8)	0.87	−0.26 (−3.0)	0.83
$0h_{9/2}$	−9.6 (−16.0)	0.86		
$1f_{7/2}$	−8.4 (−14.5)	0.87		
$1f_{5/2}$	−7.1 (−12.3)	0.87		
$2p_{3/2}$	−7.7 (−12.8)	0.88		
$2p_{1/2}$	−7.1 (−11.7)	0.88		
$0i_{13/2}$	0.79 (−4.3)	0.88		
$-E/A$	2.49 (1.52)			
r_m (fm)	4.96 (4.68)			
r_n (fm)	5.06 (4.76)			
r_c (fm)	4.87 (4.63)			

In order to obtain ^{208}Pb results corresponding to the ^{16}O and ^{40}Ca cases in which the spectrum of intermediate states with momenta between k_F and $2k_F$ is lowered to zero energy, we would have to choose $B_0 = 7\hbar\Omega$ and $\bar{N} = 54$. Our present code treats exactly $\bar{N}$ values up through 27; for higher values the shifts are only approximately taken into account and we expect the errors involved may become significant $\bar{N} \gtrsim 40$. Thus, we are forced to use shifts in ^{208}Pb which are small compared to those used in ^{16}O and ^{40}Ca. However, it can be seen from the last column in Table VI, where the entire spectrum is shifted by $7\hbar\Omega$, that it is possible to obtain binding energies in ^{208}Pb comparable to those in ^{16}O and ^{40}Ca.

Before discussing the SP levels in ^{208}Pb, let us first review some difficulties encountered in previous calculations. Figure 5 compares with experiment the high-lying neutron SP levels from (1) a HF calculation[4] using the Nestor force,[33] and (2) an unrenormalized BHF calculation[6] using Kuo's G matrix.[42] Both sets of results, which are typical of other cases,[13,32] disagree with experiment in three important ways:

(1) The main weakness is that the neutron $0i_{13/2}$ level is much too high. The same is true of the proton $0h_{11/2}$ level. Both of these levels should lie among the levels of opposite parity belonging to the oscillator shell below them; instead they are separated from the other levels by a large gap. This effect is characteristic of HF and BHF calculations for nuclei containing spin-unsaturated subshells.[13,4,6,32]

(2) The experimental SP level density is much higher than in the cases shown in Fig. 5. For both forces, the calculated levels are much too spread out. The order of magnitude of the spin-orbit splittings is about right for doublets below the Fermi surface.[43] Thus, the main problem with the level density is that the l dependence is much stronger than found experimentally.

(3) Both calculations give SP levels which are more bound than the experimental ones (except, of course, for the spin-unsaturated energies).

TABLE VI. Selected neutron SP energies and occupation probabilities, binding energy/nucleon, and charge radius for various calculations of ^{208}Pb. The dimensionality is $P+2$ with $\hbar\Omega = 9.5$. The trials listed in case A for B_0 and $\bar{N}$ pertain to proton-proton, neutron-proton, and neutron-neutron interactions, respectively; for each of the other cases single values of B_0 and of $\bar{N}$ are used with a neutron-proton $1-Q$ operator always.

Case	A	B	C	D	E
$C/\hbar\Omega$	0.0	0.0	0.0	0.0	7.0
$B_0/\hbar\Omega$	6.0, 6.5, 7.0	6.5	7.0	7.5	0.0
$\bar{N}$	26, 27, 28	27	41	41	0
$E_{0s_{1/2}}(n)$	−71.1	−70.7	−73.7	−71.1	−97.9
$E_{0p_{1/2}}(n)$	−58.8	−58.4	−61.2	−58.9	−81.2
$E_{0d_{3/2}}(n)$	−46.7	−46.5	−49.1	−47.3	−65.1
$E_{0f_{7/2}}(n)$	−34.7	−34.5	−37.1	−35.9	−50.3
$E_{0g_{7/2}}(n)$	−22.2	−22.3	−24.2	−23.8	−32.9
$E_{1d_{3/2}}(n)$	−19.3	−19.4	−21.1	−20.9	−29.2
$E_{0h_{9/2}}(n)$	−9.6	−10.1	−11.5	−12.2	−16.8
$E_{0i_{13/2}}(n)$	0.79	0.09	−1.1	−2.6	−5.3
$P_{0s_{1/2}}(n)$	0.84	0.84	0.83	0.81	0.81
$P_{0p_{1/2}}(n)$	0.84	0.84	0.82	0.80	0.80
$P_{0d_{3/2}}(n)$	0.85	0.85	0.82	0.79	0.79
$P_{0f_{7/2}}(n)$	0.85	0.85	0.82	0.78	0.78
$P_{0g_{7/2}}(n)$	0.85	0.85	0.82	0.77	0.78
$P_{1d_{3/2}}(n)$	0.86	0.85	0.82	0.78	0.78
$P_{0h_{9/2}}(n)$	0.86	0.85	0.83	0.76	0.78
$P_{0i_{13/2}}(n)$	0.88	0.87	0.84	0.78	0.79
$-E/A$	2.49	2.72	4.25	5.69	9.80
r_c (fm)	4.87	4.88	4.73	4.69	4.22

A comparison of the two calculated spectra in Fig. 5 shows fairly significant differences in the density of levels, so it is reasonable to expect difficulty (2) above might be alleviated by using other kinds of forces.[44] Also, since the inclusion of self-consistent occupation probabilities has the effect of raising the SP levels, it is clear that renormalization will help to correct difficulty (3). However, difficulty (1) appears to be more serious and, as we see in Table VI, this problem continues to persist with our present calculations.

With the above thoughts in mind, let us now examine Fig. 6, which displays all of the cases in Table VI plus case A unrenormalized. Notice for the latter that, compared to the two previous forces, the present G matrix gives levels which are not as spread out. Also, renormalization has a dramatic effect on the SP spectrum: The level density increases and the levels become less bound. The l dependence of the SP density can be

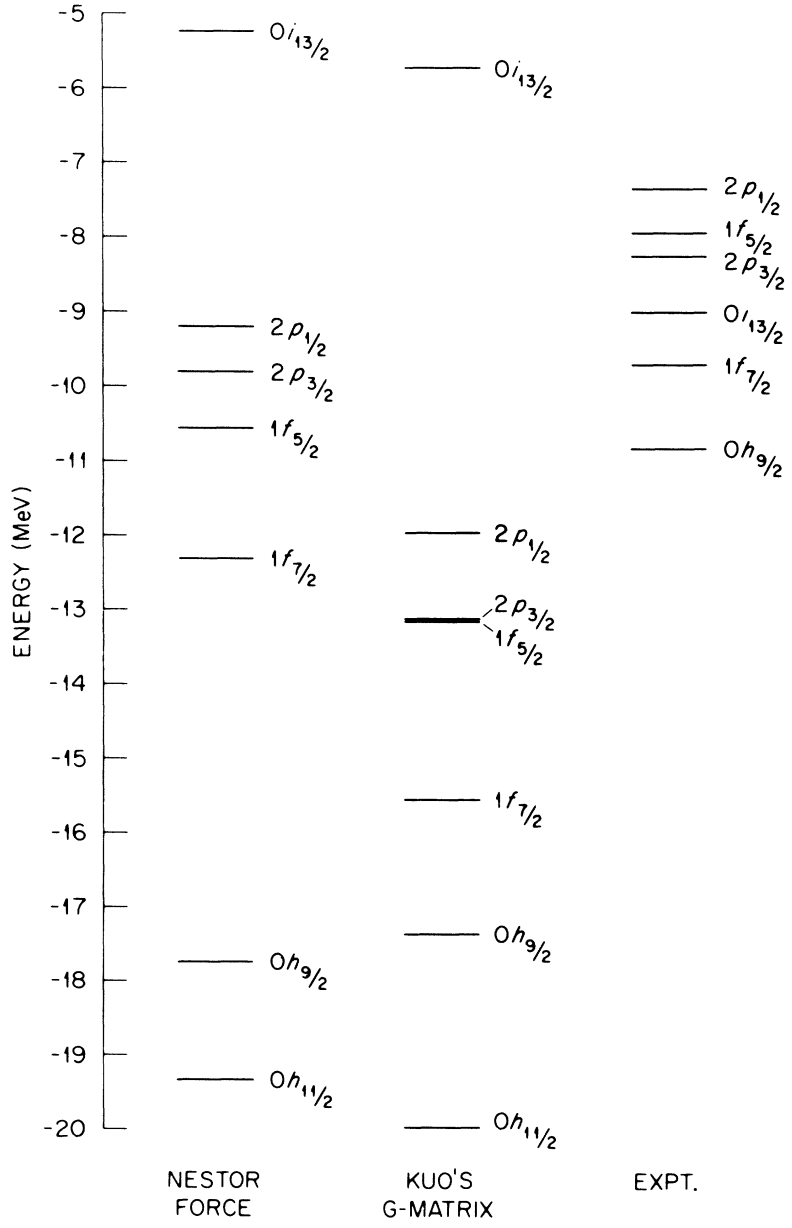

FIG. 5. Neutron SP spectra in ^{208}Pb for two previous calculations. The first column is from Ref. 4; the second column, from Ref. 6; and the experimental values, from E. Rost, Phys. Letters 26B, 184 (1968). The disagreement with experiment is much worse than for the results shown in the next figure.

improved by lowering the intermediate spectrum of the G matrix, and a comparison of cases A and B shows that using a more exact Pauli operator tends to slightly raise the energies. Case C gives reasonable agreement with experiment for the $2p$, $1f$, and $0h_{9/2}$ levels, and it is clear that by further refinements of the G matrix (improved Pauli operator and various adjustments of the intermediate spectrum) we could match these energies exactly with experiment. The point to emphasize though is that, except for the positions of the spin-unsaturated energies, the weaknesses of the previous studies can be removed by an RBHF calculation using a shifted G matrix of the type described here.

There are HF-type calculations[23-26] which do not seem to suffer from problem (1) above; i.e., the neutron $0i_{13/2}$ level is not separated from the $2p$ and $1f$ levels by a large gap. However, in these calculations various arbitrary assumptions are used, e.g., the local density approximation or an assumed one-body spin-orbit potential. These assumptions obviously simulate the effects of various higher-order diagrams needed in our work in order to bring the spin-unsaturated energies closer to experiment. It is not yet clear how these calculations avoid problem (1) or how they are related to our own work, but they do encourage us to believe that a careful study of the higher-order diagrams will be useful in solving this puzzle.

There is also the question of whether one really can compare the BHF SP energies directly with experiment. There are a number of higher-order corrections to be considered, including occupation probabilities[28] for both holes[8,12,15,19,20] and particles[44] and core polarization diagrams.[45] In our work we have treated only the occupation probabilities for hole states, and we see from Fig. 6 the dramatic improvement in the SP spectrum of ^{208}Pb. Including occupation probabilities in particle states will tend to cancel some of this improvement, but we expect this effect to be small. Core polarization diagrams do not affect the centroid of the distribution of measured SP strength but only its width.[31] Thus, if the above-mentioned corrections are the only important ones and if the experimental levels really contain 100% of the SP strength,[46] we should be able to compare our RBHF energies with experiment. However, since the spin-unsaturated levels have energies which disagree drastically with experiment, further work on this question is needed.

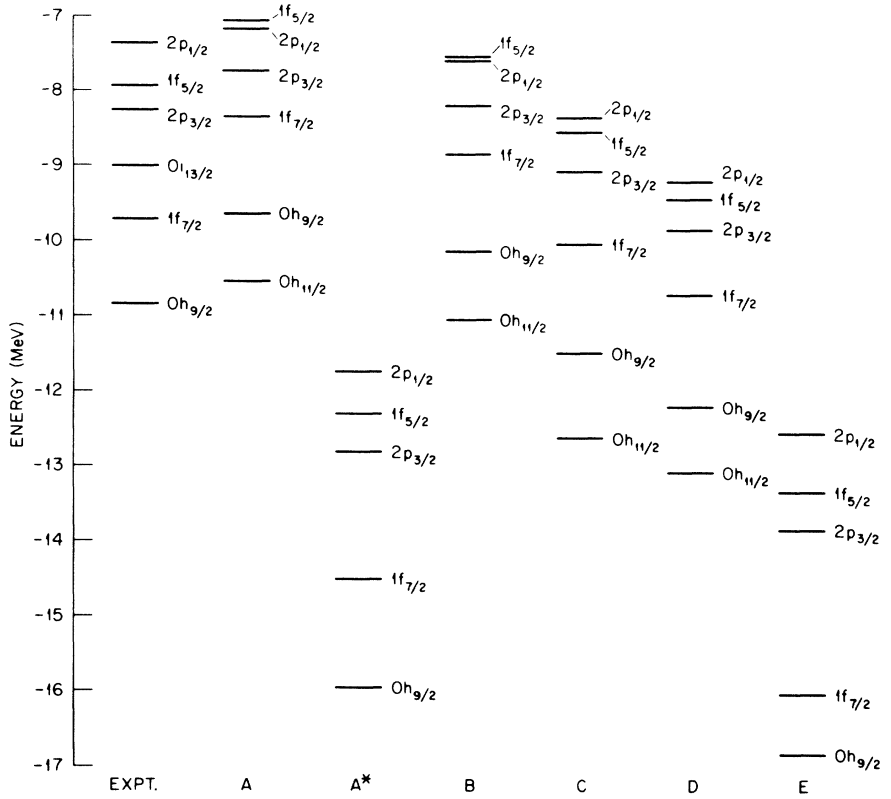

FIG. 6. High-lying neutron SP levels in ^{208}Pb for the various cases listed in Table VI. Case A* is case A unrenormalized. The experimental values are from E. Rost, Phys. Letters 26B, 184 (1968).

Finally, we should mention that our computer technology does extend to the super-heavy region, for dimensionalities as high as $D = P + 2$. In the Appendix we present some HF results, with $D = P + 1$, for the nuclei $^{310}126$ and $^{298}114$, using the Nestor force.[33] It is interesting that, in this particular case, we do not encounter the usual problem of the spin unsaturated levels. However, due to the complications associated with the SP spectrum of ^{208}Pb, we have shied away from G-matrix calculations of the super-heavy nuclei. In these nuclei it is critically important to obtain a reasonable ordering of the SP levels, and it seems pointless to go beyond ^{208}Pb with a G matrix until the problems there have been solved.

VI. SUMMARY

The results presented in Sec. V are encouraging for a number of reasons. First of all they show that accurate RBHF calculations can be carried out in the oscillator representation using dimensionalities of the same size needed for pure HF calculations. It is now possible (but, as pointed out in the last section, not yet worthwhile) to carry out RBHF calculations even for super-heavy nuclei. The results not only converge rapidly with the size of the oscillator basis but also, for a reasonable choice of intermediate-state spectrum, can be made approximately independent of the oscillator parameter.

The fact that the binding energy per particle can change by 7 or 8 MeV when the intermediate-state spectrum is shifted simply means that higher-order diagrams – in particular the three-body cluster diagrams – are important. Hopefully their contribution can be made small and independent of $\hbar\Omega$ by choosing the spectrum correctly. It is encouraging that our results are almost independent of $\hbar\Omega$ when we choose a spectrum consistent with physical intuition. Moreover, our preferred choice of intermediate-state spectrum underbinds ^{16}O and ^{40}Ca by only 1.5 MeV per particle and would probably yield similar results in ^{208}Pb if the shifts could be treated exactly.

We could, of course, easily increase the binding energy per particle by a further shift of the intermediate-state spectrum. This is illustrated in Tables IV and VI where we lower the entire particle spectrum to start at zero energy. A constant shift of this type has long been used by Becker and collaborators,[11] who have consistently obtained good binding energies for light nuclei. However, this increased shift causes a further decrease in the rms radii, which are already too small, and yields results which depend more strongly on $\hbar\Omega$.

It is not too surprising that the rms radii are all smaller than those observed experimentally, since the Reid potential does not appear to saturate nuclear matter correctly either – at least in the Brueckner approximation.[47] Our calculations are more complete than the nuclear matter calculations since we include the effect of occupation probability diagrams. These diagrams tend to improve the saturation properties, but not by a significant amount. The excellent fits to experimental binding energies, SP spectra, *and* radii found in recent HF or BHF calculations[23-27] have been obtained using effective two-body interactions containing adjustable parameters. These effective interactions usually contain nonlocal or density-dependent terms which are essential in fitting SP energy levels and helpful in improving saturation properties. Thus these terms yield effects similar to those we obtain by including occupation probability diagrams. The good fit to experimental binding energies and radii, however, comes directly from adjusting the parameters of the effective interactions to fit nuclear matter or selected finite nuclei.

It is not clear if these effective potentials merely compensate for neglected higher-order terms in the Brueckner-Goldstone expansion or if the Reid potential itself is simply not a good representation of the nucleon-nucleon interaction. In order to answer this question it is necessary to investigate higher-order corrections to the RBHF procedure.

If the three-body cluster contribution to the energy turns out to be substantially attractive, we can increase the gap between occupied and unoccupied states and thus increase the rms radius.

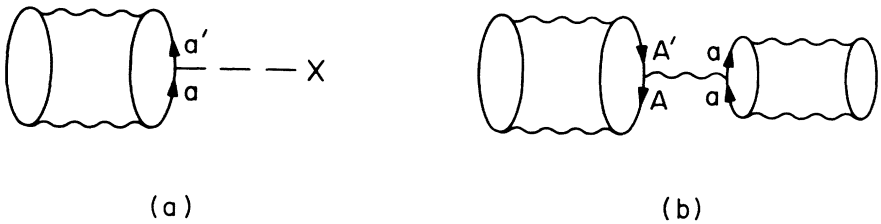

FIG. 7. Some higher-order corrections to the binding energy: (a) potential insertions in particle lines; (b) occupation probabilities for particle states.

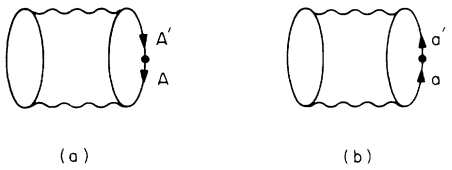

FIG. 8. (a), (b) Two-body correlation corrections to the rms radius. The dot represents the operator r^2.

As pointed out in the previous section this would have little effect on the SP spectra. Other corrections to the binding energy which should be calculated are the diagrams shown in Fig. 7, involving potential insertions in particle lines and occupation probabilities for particle states. The contributions of these diagrams should depend strongly on the particle spectrum and on $\hbar\Omega$. Thus we might have to readjust our spectrum to obtain results independent of $\hbar\Omega$. It is also possible that including occupation probabilities in particle lines could have a noticeable effect on our SP energies.

Higher-order corrections to the radius itself should also be considered. In our calculations we simply evaluate the expectation value of r^2 in lowest order. However, since the occupation probabilities of the normally occupied states are substantially less than unity, we might expect large corrections to the radius from the second-order diagrams shown in Fig. 8.[17] Diagram 8(a) alone is easy to calculate (those diagrams with $A = A'$ being proportional to $1 - P_A$) and can be shown to reduce r^2 by ~10–20%. However, diagram 8(b) is much more difficult to calculate, and both diagrams must be treated together, since they are of comparable magnitude and of opposite sign.

ACKNOWLEDGMENTS

It is a pleasure to acknowledge M. Baranger, R. L. Becker, and B. Brandow for stimulating conversations. Some of this work was carried out while one of us (R.J.M.) was an Oak Ridge Associated Universities Research Participant during the summer of 1969. We would also like to thank M. Baranger and S. J. Krieger for critically reading the original version of this manuscript and for making a number of constructive suggestions.

APPENDIX

Results for super-heavy nuclei are displayed in Table VII. For neutrons, both nuclei are calculated by filling all of the levels up through the s-d-g-i shell plus the $0j_{15/2}$ level. For protons, in $^{310}126$ all levels up through the p-f-h shell plus the $0i_{13/2}$ level are occupied, while in $^{298}114$ all of these except the $1f_{5/2}$ and $2p$ levels are assumed to be filled. The Nestor force[33] is used for the calculations, and the $\hbar\Omega$ value is chosen by extrapolating from values used in previous HF studies[4] of lower-mass nuclei. For each nucleus, the computational times on the IBM 360/91 are as follows: 25 min to calculate two-body matrix elements, and 0.9 min to perform 18 iterations.

Since the dimensionality is only $P+1$, the convergence is not very good, but the results do indicate the general trends to be expected in the super-heavy region. Notice that the $0j_{15/2}$ neutron and $0i_{13/2}$ proton levels do mix in with the levels of opposite parity in the next lowest shell, which is different from the behavior of the spin-unsaturated levels in ^{208}Pb. Also, it is interesting that in this case the $3s_{1/2}$ neutron level is separated from the other occupied neutron levels by a large

TABLE VII. HF calculations of super-heavy nuclei for the Nestor force,[33] with $\hbar\Omega = 8.30$, $l_{\text{rel}}^{(\max)} = 3$, and $D = P + 1$. The underlined SP energies for $^{298}114$ are unoccupied states. Center-of-mass corrections are not included for these nuclei.

	$^{310}126$		$^{298}114$	
	SP energies		SP energies	
SP states	Neutrons	Protons	Neutrons	Protons
$0s_{1/2}$	−102.4	−76.4	−94.5	−74.9
$0p_{3/2}$	−88.2	−63.4	−83.4	−63.5
$0p_{1/2}$	−87.7	−63.0	−83.7	−63.9
$0d_{5/2}$	−74.5	−50.5	−71.1	−51.3
$0d_{3/2}$	−73.9	−50.0	−71.3	−51.7
$1s_{1/2}$	−72.7	−48.3	−66.6	−47.8
$0f_{7/2}$	−60.4	−37.3	−57.9	−38.5
$0f_{5/2}$	−59.6	−36.6	−57.7	−38.5
$1p_{3/2}$	−55.4	−32.0	−51.1	−32.5
$1p_{1/2}$	−54.8	−31.4	−51.0	−32.6
$0g_{9/2}$	−46.2	−23.9	−44.3	−25.4
$0g_{7/2}$	−45.2	−22.9	−43.6	−24.8
$1d_{5/2}$	−39.6	−16.9	−36.4	−17.9
$1d_{3/2}$	−38.6	−16.0	−36.2	−17.9
$2s_{1/2}$	−34.8	−10.2	−30.8	−11.3
$0h_{11/2}$	−31.7	−10.0	−30.1	−11.5
$0h_{9/2}$	−29.8	−8.1	−28.5	−10.0
$1f_{7/2}$	−25.2	−3.3	−22.2	−4.3
$1f_{5/2}$	−23.5	−1.8	−21.4	3.6
$2p_{3/2}$	−19.3	4.1	−14.8	8.9
$2p_{1/2}$	−18.3	5.1	−14.0	9.8
$0i_{13/2}$	−18.4	2.6	−17.0	1.1
$0i_{11/2}$	−15.5		−14.3	
$1g_{9/2}$	−12.1		−9.6	
$1g_{7/2}$	−9.6		−7.9	
$2d_{5/2}$	−5.5		−3.0	
$2d_{3/2}$	−4.0		−2.2	
$3s_{1/2}$	2.1		3.6	
$0j_{15/2}$	−6.0		−4.6	
$-E/A$	3.83		4.02	
r_m (fm)	6.04		6.04	
r_n (fm)	6.14		6.15	
r_c (fm)	5.95		5.92	

gap. Both nuclei are bound, but there are a number of positive SP energies, particularly for $^{310}126$. Some of these characteristics could change by going to higher dimensionalities, by using improved forces, or by renormalizing with occupation probabilities.

---

*Research sponsored jointly by the U. S. Atomic Energy Commission under contract with Union Carbide Corporation, and by the National Science Foundation (Grant No. GP-13957).

†Consultant to Oak Ridge National Laboratory.

[1]R. Muthukrishnan and M. Baranger, Phys. Letters 18, 160 (1965).

[2]K. T. R. Davies, S. J. Krieger, and M. Baranger, Nucl. Phys. 84, 545 (1966).

[3]S. J. Krieger, M. Baranger, and K. T. R. Davies, Phys. Letters 22, 607 (1966).

[4]R. M. Tarbutton and K. T. R. Davies, Nucl. Phys. A120, 1 (1968).

[5]R. J. McCarthy, Nucl. Phys. A130, 305 (1969).

[6]K. T. R. Davies, M. Baranger, R. M. Tarbutton, and T. T. S. Kuo, Phys. Rev. 177, 1519 (1969).

[7]K. T. R. Davies and M. Baranger, Phys. Rev. C 1, 1640 (1970).

[8]R. J. McCarthy and K. T. R. Davies, Phys. Rev. C 1, 1644 (1970).

[9]A. K. Kerman, J. P. Svenne, and F. M. H. Villars, Phys. Rev. 147, 710 (1966).

[10]T. F. Hammann and Q. Ho-Kim, Nuovo Cimento 64B, 367 (1969); G. Saunier and J. M. Pearson, Phys. Rev. C 1, 1353 (1970); D. Gogny, P. Pires, and R. de Tourreil, Phys. Letters 32B, 591 (1970); G. Saunier and B. Rouben, to be published.

[11]A. D. MacKellar and R. L. Becker, Phys. Letters 18, 308 (1965); R. L. Becker and A. D. MacKellar, *ibid.* 21, 201 (1966); R. L. Becker, A. D. MacKellar, and B. M. Morris, Phys. Rev. 174, 1264 (1968).

[12]C. W. Wong, Nucl. Phys. A91, 399 (1967); A104, 417 (1967).

[13]C. W. Wong, Nucl. Phys. A108, 481 (1968).

[14]R. J. McCarthy and H. S. Köhler, Nucl. Phys. A99, 65 (1967).

[15]H. S. Köhler and R. J. McCarthy, Nucl. Phys. A106, 313 (1968).

[16]A. Kallio and B. D. Day, Phys. Letters 25B, 72 (1967).

[17]A. Kallio and B. D. Day, Nucl. Phys. A124, 177 (1969).

[18]D. Grillot and H. McManus, Nucl. Phys. A113, 161 (1968).

[19]R. L. Becker and B. M. Morris, Bull. Am. Phys. Soc. 13, 1363 (1968); R. L. Becker, Phys. Rev. Letters 24, 400 (1970); R. L. Becker, Phys. Letters 32B, 263 (1970).

[20]R. L. Becker and K. T. R. Davies, in *Proceedings of the International Conference on Properties of Nuclear States, Montreal, Canada, 1969,* edited by M. Harvey *et al.* (Presses de l'Université de Montréal, Montréal, Canada, 1969).

[21]R. L. Becker, K. T. R. Davies, and M. R. Patterson, to be published.

[22]J. M. Irvine, Nucl. Phys. A120, 576 (1968).

[23]J. W. Negele, Phys. Rev. C 1, 1260 (1970).

[24]D. M. Brink and D. Vautherin, in *Proceedings of the International Conference on Properties of Nuclear States, Montreal, Canada, 1969,* edited by M. Harvey *et al.* (Presses de l'Université de Montréal, Montréal, Canada, 1969); D. Vautherin and D. M. Brink, Phys. Letters 32B, 149 (1970).

[25]J. Nemeth and D. Vautherin, Phys. Letters 32B, 561 (1970).

[26]H. S. Köhler and Y. C. Lin, Nucl. Phys. A136, 35 (1969); H. S. Köhler, Nucl. Phys. A144, 407 (1970); H. S. Köhler, Nucl. Phys. A162, 385 (1971); H. S. Köhler and Y. C. Lin, to be published.

[27]S. A. Moszkowski, Phys. Rev. C 2, 402 (1970); this paper contains a short review of many earlier calculations using effective interactions.

[28]B. H. Brandow, Phys. Rev. 152, 863 (1966); Rev. Mod. Phys. 39, 771 (1967); in *Proceedings of the Lectures in Theoretical Physics,* edited by K. T. Mahanthappa (Gordon and Breach, Science Publishers, Inc., New York, 1969), Vol. XI; Ann. Phys. (N.Y.) 57, 214 (1970).

[29]R. V. Reid, Ann. Phys. (N.Y.) 50, 411 (1968).

[30]T. Hamada and I. D. Johnston, Nucl. Phys. 34, 382 (1962).

[31]M. Baranger, Nucl. Phys. A149, 225 (1970).

[32]D. Vautherin and M. Veneroni, Phys. Letters 29B, 203 (1969).

[33]C. W. Nestor, K. T. R. Davies, S. J. Krieger, and M. Baranger, Nucl. Phys. A113, 14 (1968).

[34]H. A. Bethe, B. H. Brandow, and A. G. Petschek, Phys. Rev. 129, 225 (1963).

[35]M. Baranger, in *Nuclear Structure and Nuclear Reactions, Proceedings of the International School of Physics "Enrico Fermi," Course XL, Varenna, 1967,* edited by M. Jean and R. A. Ricci (Academic Press Inc., New York, 1969).

[36]S. A. Coon and J. Dabrowski, Phys. Rev. 140B, 287 (1965).

[37]P. H. W. Kao, Ph.D. thesis, Carnegie-Mellon University, 1969 (unpublished); P. H. W. Kao, J. Depp, R. J. McCarthy, and M. Baranger, in *Proceedings of the International Conference on Properties of Nuclear States, Montreal, Canada, 1969,* edited by M. Harvey *et al.* (Presses de l'Université de Montréal, Montréal, Canada, 1969).

[38]B. R. Barrett, R. G. L. Hewitt, and R. J. McCarthy, to be published.

[39]K. T. R. Davies and R. L. Becker, to be published.

[40]A. H. Wapstra, Physica 21, 385 (1955).

[41]H. R. Collard, L. R. B. Elton, and R. Hofstadter, in *Landolt-Börnstein Numerical Data and Functional Relationships in Science and Technology,* edited by K.-H. Hellwege and H. Schopper (Springer-Verlag, Berlin, Germany, 1967).

[42]T. T. S. Kuo, Nucl. Phys. A103, 71 (1967).

[43]T. T. S. Kuo, private communication.

[44]M. Baranger, private communication.

[45]G. F. Bertsch and T. T. S. Kuo, Nucl. Phys. A112, 204 (1968).

[46]G. E. Brown, Comments Nucl. Particle Phys. 3, 136 (1969).

[47]P. J. Siemens, Nucl. Phys. A141, 225 (1970).